

Space-time crystal and space-time group symmetry

Shenglong Xu and Congjun Wu

Department of Physics, University of California, San Diego, California 92093, USA

Crystal structures and the Bloch theorem play a fundamental role in condensed matter physics. We propose “space-time” crystals exhibiting the general intertwined space-time periodicities in $D+1$ dimensions, which include the Floquet lattice systems as a special case. Their crystal symmetry structures are described by “space-time” groups. Compared to space and magnetic groups, they are augmented by “time-screw” rotations and “time-glide” reflections involving fractional time translations. A complete classification of the 13 space-time groups in 1+1D is performed. Kramers-type degeneracy can arise from space-time symmetries without the half-integer spinor structure, which constrains the winding number patterns of spectral dispersions. In 2+1D, non-symmorphic space-time symmetries enforce spectral degeneracies, leading to protected Floquet semi-metal states. Our work provides a general framework for further studying topological properties of the $D + 1$ dimensional space-time crystals.

PACS numbers:

The fundamental concept of energy bands in crystals based on the Bloch theorem lays the foundation of modern condensed matter physics. In the past decade, studies on band structure symmetry and topology lead to important discoveries of the topological insulating state, topological superconductivity, and the Weyl semi-metal state [1–3]. More recently, periodically driven systems have also attracted increasing interests. Periodic driving provides a new route to engineer topological states in systems originally topologically trivial in the absence of driving. Such possibilities have been explored in various systems, including the irradiated graphene [4, 5], semiconducting quantum wells [6], dynamically modulated cold atom optical lattices [7], and photonic systems [8, 9]. For driven systems with a temporal period T , Bloch bands are replaced by Bloch-Floquet bands, which are periodic in energy space since the quasi-energy is only conserved module $2\pi/T$. This feature further enriches topological band structures [10–12]. For non-interacting systems, this extra periodicity leads to the dynamically generated Majorana modes in 1D [13], and anomalous edge states with zero Chern number in 2D [14]. Topological classifications for interacting Floquet systems have also been investigated [15–19].

Symmetry plays a fundamental role in analyzing topological properties of periodically driven systems. However, previous studies mostly treat the temporal periodicity separated from the spatial one. In fact, the driven system can exhibit much richer symmetry structures than a simple direct product of symmetries in space and time domains. In particular, a temporal translation at a *fractional* period can be combined with space group symmetries to form novel space-time intertwined symmetries, which, to the best of our knowledge, have not yet been fully explored. For static lattices, the intrinsic connections between the space-group symmetries and physical properties, especially the topological phases, have been extensively studied [20–24]. Therefore, it is expected that

the intertwined space-time symmetries could also protect novel trivial properties of the driven system, regardless of microscopic details.

In this article, we generalize the concept of Floquet-Bloch lattices to space-time crystals, which exhibit intertwined space-time symmetries. Space-time crystals exhibit the periodicities characterized by $D + 1$ linearly independent basis vectors, which are space-time mixed in general. The usual Floquet-Bloch systems are a special case exhibiting separate spatial and temporal periodicities. The full discrete space-time symmetries of space-time crystals form groups – dubbed “space-time” groups, which are generalizations of space groups for static crystals by including “time-screw” and “time-glide” operations. A complete classification of the 13 space-time groups in 1+1 D is performed, and their constraints on band structure winding numbers are studied. In 2+1 D, the non-symmorphic space-time symmetry operations, similar to their static space-group counterparts, lead to spectral degeneracies for periodically driven systems, even when the instantaneous spectra are gapped at any given time t .

Space-time lattice – We consider the time-dependent Hamiltonian $H = P^2/(2m) + V(\mathbf{r}, t)$ in the $D + 1$ dimensional space-time. $V(\mathbf{r}, t)$ exhibits the intertwined discrete space-time translational symmetry as

$$V(\mathbf{r}, t) = V(\mathbf{r} + \mathbf{u}^i, t + \tau^i), \quad i = 1, 2, \dots, D + 1, \quad (1)$$

where $(\mathbf{u}^i, \tau^i) = a^i$ is the primitive basis vector of the space-time lattice. Eq. 1 extends the usual Floquet-Bloch lattice with the separated spatial and temporal periodicities to the more general case with space-time mixed primitive vectors. In general, the space-time primitive unit cell is not a direct product between spatial and temporal domains. There may not even exist spatial translational symmetry at any given time t , nor temporal translational symmetry at any spatial location \mathbf{r} . Consequently, the frequently used time-evolution opera-

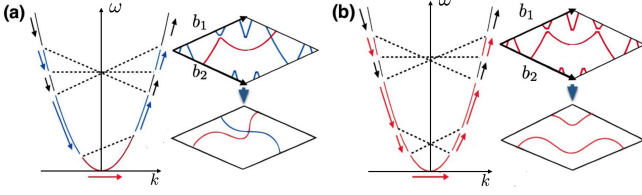


FIG. 1: Folding the band dispersions of the 1+1 D space-time crystal into the 1st rhombic MEBZ in the weak lattice limit. The momentum-energy reciprocal lattice vectors of nonzero V_B 's are represented by dashed lines. The low-energy part of the free dispersion curve evolves to closed loops. (a) Two loops with the winding numbers $\mathbf{w}_r = (1, 0)$ (red) and $\mathbf{w}_b = (0, 1)$ (blue). (b) An extra nonzero V_G connects two loops in (a) forming a new one with $\mathbf{w} = \mathbf{w}_r + \mathbf{w}_b$.

tor $U(T)$ of one period for the Floquet problem generally does not apply. The reciprocal lattice is spanned by the momentum-energy basis vectors $b^i = (\mathbf{G}^i, \Omega^i)$ defined through $b^i \cdot a^j = \sum_{m=1}^D G_m^i u_m^j - \Omega^i \tau^j = 2\pi \delta^{ij}$. The $D+1$ dimensional momentum-energy Brillouin zone (MEBZ) may also be momentum-energy mixed.

We generalize the Floquet-Bloch theorem for the time-dependent Schrödinger equation $i\hbar \partial_t \psi(\mathbf{r}, t) = H(\mathbf{r}, t) \psi(\mathbf{r}, t)$. Due to the space-time translation symmetry, the lattice momentum-energy vector $\kappa = (\mathbf{k}, \omega)$ is conserved. Only the κ vectors inside the first MEBZ are non-equivalent, and the κ vectors outside are equivalent to those inside up to integer reciprocal lattice vectors. The states characterized by κ take the form of

$$\psi_{\kappa, m}(\mathbf{r}, t) = e^{i(\mathbf{k} \cdot \mathbf{r} - \omega_m t)} u_m(\mathbf{r}, t), \quad (2)$$

where m marks different states sharing the common κ . $u_m(\mathbf{r}, t)$ processes the same space-time periodicity as $H(\mathbf{r}, t)$, and is expanded as $u_m = \sum_B c_{m, B} e^{i(\mathbf{G} \cdot \mathbf{r} - \Omega t)}$ with $B = (\mathbf{G}, \Omega)$ taking all the momentum-energy reciprocal lattice vectors. The eigen-frequency ω_m is determined through the eigenvalue problem defined as

$$\sum_{B'} \{[-\Omega + \varepsilon_0(\mathbf{k} + \mathbf{G})] \delta_{B, B'} + V_{B-B'}\} c_{m, B'} = \omega_m c_{m, B}, \quad (3)$$

where $\varepsilon_0(\mathbf{k})$ is the free dispersion, and V_B is the momentum-energy Fourier component of the space-time lattice potential $V(\mathbf{r}, t)$. The dispersion based on Eq. 3 is represented by a D -dimensional surface in the MEBZ which is a $D+1$ dimensional torus.

The energy band structures of the space-time lattice exhibit novel features different from those with separated spatial and temporal periodicities. For simplicity, below we use the 1+1 D case to investigate the symmetry and topological properties of the space-time crystal.

Dispersion winding numbers – The dispersion relation $\omega(k)$ forms closed loops in the 2D toroidal MEBZ, each of which is characterized by a pair of winding numbers

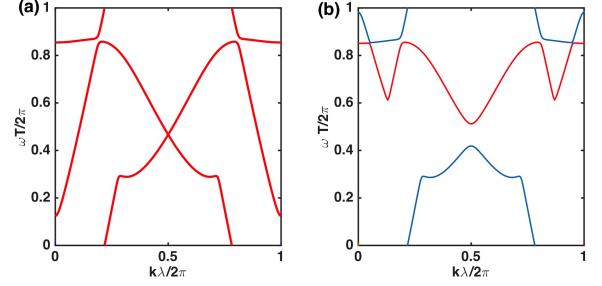


FIG. 2: (a) The Floquet-Bloch band spectrum with the space-time lattice potential possessing the glide time-reflection symmetry g_t . When applied to the states with $\kappa_x = \pi/\lambda$, g_t becomes a Kramers symmetry protecting the double-degeneracy. (b) Lifting the Kramers degeneracy by adding a time-glide-reflection symmetry breaking term.

$\mathbf{w} = (w_1, w_2)$. Compared to the static lattice case in which the band dispersion only winds around the momentum direction, here $\omega(k)$ is typically not single-valued and its winding patterns are much richer. The dispersions in the limit of a weak space-time potential $V(x, t)$ with a rhombic MEBZ are illustrated in Fig. 1 (a) and (b). When folded into the MEBZ, the free dispersion curve $\varepsilon(k)$ can cross at general points not just on high symmetry ones. A crossing point corresponds to two equivalent momentum-energy points related by a reciprocal vector G before folding. When $V_G \neq 0$, the crossing is avoided by forming a gap at the magnitude of $2|V_G|$. The winding directions of the dispersion loops are generally momentum-energy mixed. Furthermore, different momentum-energy reciprocal lattice vectors can cross each other, leading to composite loops winding around the MEBZ along both directions as shown in Fig. 1 (b). The total number of states at each \mathbf{k} is invariant with lattice potential, then crossing can only split along the ω -direction and $d\omega/dk$ is always finite. Consequently, trivial loops with the winding numbers $(0, 0)$ are forbidden, while all other patterns (w_1, w_2) are possible in general.

The intertwined space-time lattice symmetries besides translations can protect crossings and impose further constraints on band structures. Consider a 1+1 D crystal structure with the space-time unit cell as the direct product of spatial and temporal periods λ and T , respectively. Its first MEBZ is also a direct-product as $[-\pi/\lambda, \pi/\lambda] \otimes [-\pi/T, \pi/T]$. We further assume the system is invariant under a combined time-reversal transformation followed by the translation of a half spatial period. This operation denoted as g_t can be viewed as a “glide time-reflection” defined as $g_t(x, t) = (x + \frac{1}{2}\lambda, -t)$. Its operation on the Hamiltonian is defined as $g_t^{-1} H g_t = H^*(g_t(x, t))$. The corresponding transformation M_{g_t} on the Bloch-Floquet wavefunction $\psi_\kappa(x, t)$ of Eq. 2 is anti-unitary defined as $M_{g_t} \psi_\kappa = \psi_\kappa^*(g_t^{-1}(x, t))$. The glide time-reflection leaves the line of $\kappa_x = \pi/\lambda$ in the MEBZ

invariant. M_{g_t} becomes a Kramers symmetry for states along this line,

$$M_{g_t}^2 \psi_\kappa = \psi_\kappa(x - \lambda, t) = e^{-i\kappa_x \lambda} \psi_\kappa = -\psi_\kappa, \quad (4)$$

which arises purely from the space-time crystal symmetry without involving the half-integer spinor structure. It protects the double degeneracy of the momentum-energy quantum numbers of ψ_κ and $M_{g_t} \psi_\kappa$. Hence the crossing at $\kappa_x = \pi/\lambda$ cannot be avoided and the dispersion winding numbers along the momentum direction must be even.

As a concrete example, we study a crystal potential with the above spatial and temporal periodicities, $V(x, t) = V_0 \left(\sin \frac{2\pi}{T} t \cos \frac{2\pi}{\lambda} x + \cos \frac{2\pi}{T} t \right)$. Except the glide time-reflection symmetry, it does not possess other space-time symmetries. Its Bloch-Floquet spectrum is calculated based on Eq. 3, and a representative dispersion loop is plotted in the MEBZ shown in Fig. 2 (a). The crossing at $\kappa_x = \pi/\lambda$ is protected by the glide time-reflection symmetry giving rise to a pair of Kramers doublet. As a result, the winding number of this loop is $\mathbf{w} = (w_x, w_t) = (2, 0)$. If a glide time-reflection symmetry breaking term $\delta V = V_0' \cos(\frac{2\pi}{\lambda} x)$ is added into the crystal potential, the crossing is avoided due to the Kramers symmetry breaking as shown in Fig. 2 (b). Consequently, the dispersion splits into two loops, both of which exhibit the winding number $(1, 0)$.

Space-time group – We propose the concept of “space-time” group for a full description of the symmetry properties of the $D + 1$ dimensional space-time crystal structures. It not only includes space group and magnetic group transformations in the D -spatial dimensions, but also is extended to include operations involving fractional translations along the time-direction. Since space and time are non-equivalent in the Schrödinger equation, space-time rotations are not allowed except the 2-fold case. For a symmetry operation Γ of the space-time crystal, its operation on (\mathbf{r}, t) is defined as,

$$\Gamma(\mathbf{r}, t) = (R\mathbf{r} + \mathbf{u}, st + \tau), \quad (5)$$

where R is a D -dimensional point group operation, $s = \pm 1$ and $s = -1$ indicates time-reflection, *i.e.*, time-reversal, and $(\mathbf{u}, \tau) = \sum_i m_i a^i$ represents a space-time translation with m_i either integers or fractions. At $\tau = 0$, Γ is reduced to a space group or magnetic group operation according to $s = \pm 1$, respectively. At $\tau \neq 0$, when (\mathbf{u}, τ) contains fractions of a^i , new symmetry operations arise due to the dynamic nature of the crystal potential, including the “time-screw” rotation and “time-glide” reflection, which are a spatial rotation or a reflection followed by a fractional time translation, respectively. The operation of Γ on the Hamiltonian is defined as $\Gamma^{-1} H(\mathbf{r}, t) \Gamma = H(\Gamma(\mathbf{r}, t))$, or, $\Gamma^{-1} H(\mathbf{r}, t) \Gamma = H^*(\Gamma(\mathbf{r}, t))$ for $s = \pm 1$, respectively. Correspondingly, the transformation M_Γ on the Bloch-Floquet wavefunctions $\psi_\kappa(\mathbf{r}, t)$

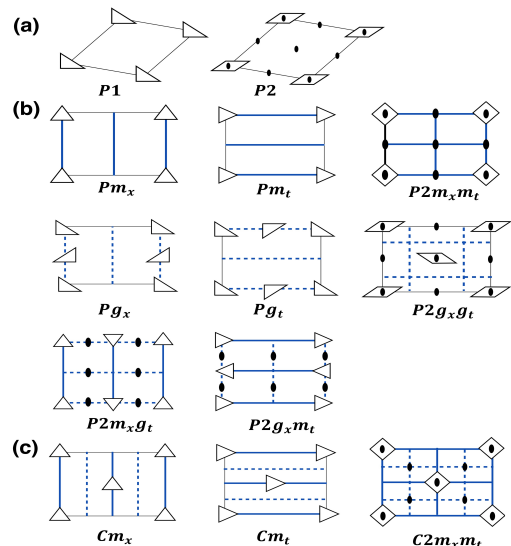


FIG. 3: The classification of 13 space-time groups in 1+1D and the associated lattice configurations. The solid oval marks the 2-fold space-time axis, and the parallelogram mean the 2-fold axis without reflection symmetries. The thick solid and dashed lines represent reflection and glide-reflection axes, respectively. Configurations of triangles and the diamond denote the local symmetries under reflections. (a) The oblique lattices with and without 2-fold axes. Their basis vectors are generally space-time mixed. The primitive (b) and centered (c) orthorhombic lattices: According to their reflection and glide reflection symmetries, they are classified to 8 groups in (b), and 3 groups in (c).

is $M_\Gamma \psi_\kappa = \psi_\kappa(\Gamma^{-1}(\mathbf{r}, t))$, or, $\psi_\kappa^*(\Gamma^{-1}(\mathbf{r}, t))$ for $s = \pm 1$, respectively.

As a concrete example, we present a complete classification of the space-time groups for 1+1 D space-time crystal structures. Due to the non-equivalence between spatial and temporal directions, there are no square and hexagonal space-time crystal systems. The point-group like operations are isomorphic to D_2 , including reflection m_x , time reversal m_t , and their combination $m_x m_t$, *i.e.*, the 2-fold space-time rotation. Consequently, only two space-time crystal systems are allowed – oblique and orthorhombic. In addition to g_t , symmetries involving fractional translations also include the “time glide reflection” g_x - spatial reflection followed by a fractional time-translation. The space-time crystal structures marked with m_x and m_t , or those with g_x and g_t , should be different, respectively.

The above 1+1 D space-time symmetries give rise to 13 space-time groups in contrast to the 17 wallpaper space groups characterizing the 2D static lattices. The oblique Bravais lattice is simply monoclinic, while the orthorhombic ones include both the primitive and centered Bravais lattices. The monoclinic lattice gives rise to two different crystal structures with and without the 2-fold space-time axes, whose space-time groups are denoted by

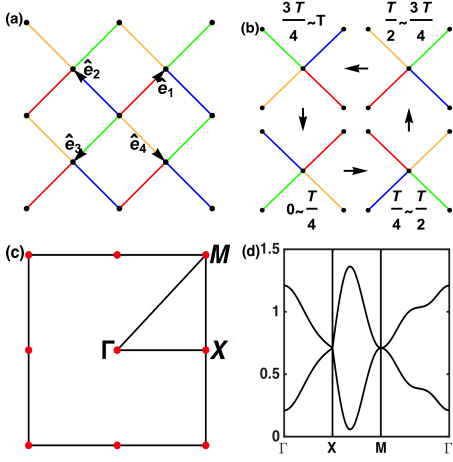


FIG. 4: (a) The 2+1 D space-time lattice structure of the Hamiltonian Eq. 7. The bond directions are marked as $\vec{e}_{1,3} = \pm\frac{1}{2}(\hat{x} + \hat{y})$, $\vec{e}_{2,4} = \mp\frac{1}{2}(\hat{x} - \hat{y})$. (b) The time-dependent hopping pattern rotates 90° every one quarter period. The bonding strengths $w_{e_i}(t)$ of the R , B , G and Y bonds equal 0.2, 3, -3.2 , and 0.5, respectively. (c) The momentum Brillouin zone with high symmetry points $\Gamma = (0, 0)$, $M = (\pm\pi, \pm\pi)$, and $X = (0, \pm\pi)$ and $(\pm\pi, 0)$. (d) The dispersions along the cuts from Γ to X to M to Γ . Two-fold degeneracies appear at X and M .

$P_{1,2}$, respectively, as shown in Fig. 3 (a). For the primitive orthorhombic lattices, the associated crystal structures can exhibit the point-group symmetries m_x and m_t , and the space-time symmetries g_t and g_x . Their combinations give rise to crystal structures with 8 space-time group symmetries denoted as Pm_x , Pm_t , $P2m_xm_t$, Pg_x , Pg_t , $P2g_xg_t$, $P2m_xg_t$, $P2g_xm_t$, respectively, as shown in Fig. 3 (b). Four of them possess the 2-fold space-time axes as indicated by “2” in their symbols. For the centered orthorhombic Bravais lattices, 3 crystal structures exist with space-time groups denoted as Cm_x , Cm_y , and $C2m_xm_t$, respectively, as shown in Fig. 3 (c). They all exhibit glide-reflection symmetries, and the last one possesses the 2-fold space-time axes as well. Two unit cells are plotted for the centered lattices to show the full symmetries explicitly, and their primitive basis vectors are actually space-time mixed.

The 2+1 D space-time crystals. - The classifications of the space-time groups in more than 1+1 D are generally complicated. The 2+1D case is analyzed in Supplementary Material, whose structures are further enriched by spatial rotations and time-screw rotations.

Below we show that the space-time group operations protect robust spectrum degeneracies and lead to the Floquet semi-metal state by using a 2+1D example. Consider the case that the space-time little group of the momentum \mathbf{k} contains two non-symmorphic space-time group operations $g_{1,2}$ satisfying

$$g_1g_2 = T(\mathbf{u})g_2g_1, \quad \text{and,} \quad \mathbf{k} \cdot \mathbf{u} = 2\pi p/q, \quad (6)$$

where $T(\mathbf{u})$ is a space translation of integer lattice vectors, and p and q coprime. We find that the Bloch-Floquet wavefunctions exhibit a q -fold degeneracy at the momentum-energy vector $\kappa = (\mathbf{k}, \omega)$ proved as follows. Since g_1 belongs to the little group, $\psi_\kappa(\mathbf{r}, t)$ can be chosen to satisfy $M_{g_1}\psi_{\kappa,1} = \mu\psi_{\kappa,1}$, then $\psi_\kappa, M_{g_2}\psi_\kappa, M_{g_2}^2\psi_\kappa, \dots, M_{g_2}^{q-1}\psi_\kappa$ are the common Bloch-Floquet eigenstates sharing the same κ but exhibiting a set of different eigenvalues of g_1 as $\eta, \mu\eta, \mu\eta^2, \dots, \mu\eta^{q-1}$ with $\eta = e^{i\pi p/q}$. Then they are orthogonal to each other forming a q -fold degeneracy. Compared to the case of non-symmorphic space group protected degeneracy [21, 22, 24], here $g_{1,2}$ are space-time operations for a dynamic space-time crystal.

We employ a 2+1 D tight-binding space-time model as an example to illustrate the above protected degeneracy. A snap shot of the lattice is depicted in Fig. 4 (a), which consists of two sublattices: The A -type sites are with integer coordinates (i, j) , and each A -site emits four bonds along \vec{e}_i to its four neighboring B sites at $(i \pm \frac{1}{2}, j \pm \frac{1}{2})$. The space-time Hamiltonian within the period T is

$$H(t) = - \sum_{\vec{r} \in A, \vec{r} + \frac{a}{2}\vec{e}_i \in B} \{w_{\vec{e}_i}(t)c_{\vec{r}}^\dagger d_{\vec{r} + \frac{a}{2}\vec{e}_i} + h.c.\}, \quad (7)$$

where a is the distance between two nearest A sites, and $w_{\vec{e}_i}(t)$'s are hopping amplitudes with different strengths. Their time-dependence is illustrated in Fig. 4 (b): Within each quarter period, $w_{\vec{e}_i}$ does not vary, and their pattern rotates 90° after every $T/4$. At each given time, the lattice possesses a simple 2D space group symmetry $p2111$, which only includes two-fold rotations around the AB -bond centers without reflection and glide-plane symmetries. For example, the rotation R_π around $(\frac{a}{4}, \frac{a}{4})$ transforms the coordinate $(x, y, t) \rightarrow (\frac{a}{2} + x, \frac{a}{2} + y, t)$. In addition, there exist “time-screw” operations, say, an operation S defined as a rotation around an A -site $(0, 0)$ at 90° followed by a time-translation at $T/4$, which transforms $(x, y, t) \rightarrow (y, -x, t + \frac{T}{4})$. R_π and S are generators of the space-time group for Eq. 7. Since S is a time-screw rotation, this space-time group is non-symmorphic. It is isomorphic to the 3D space-group $I4_1$, while its 2D space subgroup $p2111$ is symmorphic. We have checked that, for a static Hamiltonian taking any of the bond configuration in Fig. 4 (b), the energy spectra are fully gapped. However, the non-symmorphic space-time group gives rise to spectral degeneracies. Its momentum Brillouin zone is depicted in Fig. 4 (c). The space-time little group of the M -point (π, π) contains both R and S satisfying $RS = T(a\hat{y})SR = -SR$. Similarly, the X -point $(\pi, 0)$ is invariant under both R and S^2 satisfying $RS^2 = T(a\hat{x} + a\hat{y})S^2R = -S^2R$. Hence, the Floquet eigen-energies are doubly degenerate at M and X -points as shown in Fig. 4 (d), showing a semi-metal structure.

In conclusion, we have studied a novel class of $D+1$ dimensional crystal structures exhibiting the general space-time periodicities. Their momentum-energy Brillouin

zones are $D + 1$ dimensional torus and are typically momentum-energy entangled. The band dispersions exhibit non-trivial windings around the momentum-energy Brillouin zones. The space-time crystal structures are classified by the “space-time” symmetry groups, which extend the space group for static crystal structures by incorporating “time-screw” rotations and “time-glide” reflections. In 1+1D, a complete classification of the 13 space-time groups is performed. Space-time symmetries give rise to novel Kramers degeneracy independent of the half-integer spinor structure. The non-symmorphic space-time group operations lead to protected spectral degeneracies for the 2+1 D space-time lattices.

S. X. and C.W. are supported by the NSF DMR-1410375 and AFOSR FA9550-14-1-0168.

-
- [1] M. Z. Hasan and C. L. Kane, *Rev. Mod. Phys.* **82**, 3045 (2010).
- [2] X.-L. Qi and S.-C. Zhang, *Rev. Mod. Phys.* **83**, 1057 (2011).
- [3] C. K. Chiu, J. C. Y. Teo, A. P. Schnyder, and S. Ryu, *Rev. Mod. Phys.* **88**, 1 (2016).
- [4] T. Oka and H. Aoki, *Phys. Rev. B* **79**, 081406 (2009).
- [5] Z. Gu, H. A. Fertig, D. P. Arovas, and A. Auerbach, *Phys. Rev. Lett.* **107**, 216601 (2011).
- [6] N. H. Lindner, G. Refael, and V. Galitski, *Nat. Phys.* **7**, 490 (2011).
- [7] G. Jotzu *et al.*, *Nature* **515**, 237 (2014).
- [8] M. C. Rechtsman *et al.*, *Nature* **496**, 196 (2013).
- [9] D. Leykam, M. C. Rechtsman, and Y. D. Chong, *Phys. Rev. Lett.* **117**, 013902 (2016).
- [10] T. Kitagawa, E. Berg, M. Rudner, and E. Demler, *Phys. Rev. B* **82**, 235114 (2010).
- [11] J. K. Asbóth, B. Tarasinski, and P. Delplace, *Phys. Rev. B* **90**, 125143 (2014).
- [12] R. Roy and F. Harper, arXiv:1603.06944 (2016).
- [13] M. Thakurathi, A. A. Patel, D. Sen, and A. Dutta, *Phys. Rev. B - Condens. Matter Mater. Phys.* **88**, 155133 (2013).
- [14] M. S. Rudner, N. H. Lindner, E. Berg, and M. Levin, *Phys. Rev. X* **3**, 031005 (2013).
- [15] A. C. Potter and T. Morimoto, arXiv:1610.03485 (2016).
- [16] A. C. Potter, T. Morimoto, and A. Vishwanath, *Phys. Rev. X* **6**, 041001 (2016).
- [17] C. W. Von Keyserlingk and S. L. Sondhi, *Phys. Rev. B - Condens. Matter Mater. Phys.* **93**, 245145 (2016).
- [18] C. W. von Keyserlingk and S. L. Sondhi, *Phys. Rev. B* **93**, 245146 (2016).
- [19] D. V. Else and C. Nayak, *Phys. Rev. B - Condens. Matter Mater. Phys.* **93**, 201103 (2016).
- [20] L. Fu, *Phys. Rev. Lett.* **106**, 106802 (2011).
- [21] S. A. Parameswaran, A. M. Turner, D. P. Arovas, and A. Vishwanath, *Nat. Phys.* **9**, 299 (2013).
- [22] S. M. Young and C. L. Kane, *Phys. Rev. Lett.* **115**, 126803 (2015).
- [23] Z. Wang, A. Alexandradinata, R. J. Cava, and B. A. Bernevig, *Nature* **532**, 189 (2016).
- [24] H. Watanabe, H. C. Po, M. P. Zaletel, and A. Vishwanath, *Phys. Rev. Lett.* **117**, 096404 (2016).